5
Biomass Burning Fuel Consumption and Emissions for Air Quality

Nancy H. F. French[1] and Andrew T. Hudak[2]

ABSTRACT

Biomass burning emissions estimates of gas and aerosol air pollutants are used in modeling and forecasting smoke and air quality. These emissions originate from combustion of the fuels found in the landscape and vary based on the terrain, weather, fuel type, and condition of the fuelbed, including the arrangement of fuels, during the fire event. Combustion describes the flaming and smoldering burning phases of a fire that, summed over the duration of the event, equals the fuel consumed. This chapter provides a review of approaches to quantify fuel consumption from biomass burning relevant for air quality assessment. The indirect approach estimates consumption based on the difference between pre- and post-fire fuel loads within the burn area or models it by applying a burning efficiency to the pre-fire fuel load. The direct approach uses a combustion factor to translate fire radiative power (FRP) measured from thermal infrared instruments into the consumption rate; temporally integrating FRP over the duration of the fire provides fire radiative energy (FRE), which the same combustion factor translates to total consumption. Methods to map the location, strength, and composition of fire emissions, which are a function of fuel characteristics and fire environment, are provided. This chapter provides a discussion on the uncertainty of biomass burning emissions inventory products and considers new approaches for improving fuel consumption mapping.

5.1. INTRODUCTION

Emissions from biomass burning are the direct product of the consumption of fuels during fire, made up of the live and dead vegetation found in the landscape (Ottmar, 2014). The process is fuels driven and mediated by weather and topography to create spatial-temporal complexity in how and where fuels burn and the resulting emissions. The combustion process produces energy (heat and light), gases, and solids of various sizes that are either left as residue at the site (ash and char) or lofted into the air as particulate matter (PM), an important component of smoke. A variety of different gaseous and particulate combustion products are emitted into the atmosphere depending on the fuel type and conditions during burning, including the fuel moisture, arrangement of fuels, terrain, and fire weather, which influence the intensity and efficiency of burning (Prichard et al., 2020).

Global carbon emissions from biomass burning have been estimated to average 2,200 TgC yr^{-1} from 1997 to 2016, and extend as high as 3,000 TgC in 1 yr (1997) (van der Werf et al., 2017), with high interannual variation. Additionally, differences are found between studies, depending on the approach (Hoelzemann et al., 2004; Ito & Penner, 2004; van der Werf et al., 2006). In years since

[1]*Michigan Tech Research Institute, Michigan Technological University, Ann Arbor, Michigan, USA*

[2]*Forestry Sciences Laboratory, Rocky Mountain Research Station, United States Forest Service, Moscow, Idaho, USA*

Landscape Fire, Smoke, and Health: Linking Biomass Burning Emissions to Human Well-Being, Geophysical Monograph 280, First Edition.
Edited by Tatiana V. Loboda, Nancy H. F. French, and Robin C. Puett.

DOI: 10.1002/9781119757030.ch05

these studies, several regions have experienced unprecedented levels of fire, so these data from the late 1990s and early 2000s should be considered an illustration of the complexity of the question "How much pollution does biomass burning contribute to the atmosphere?" Improving estimates of the magnitude and composition of biomass burning emissions has gained attention since 2000, pointing to the growing concern to better understand biomass burning emissions for both climate and air quality (Larkin et al., 2020).

An emissions inventory is a periodically generated accounting (e.g., hourly, daily, annual) of the amount of pollutants released into the atmosphere from a source. Emissions inventories can be used as input to atmospheric models to map the concentrations of smoke in the atmosphere (see Chapters 7–9), or by land and air quality managers to assess expected emissions impacts on air quality, visibility, and health, or in carbon cycle modeling and management (e.g., Gurney et al., 2020; Pouliot et al., 2008). Within the context of this book, the focus of this chapter is on emissions of pollutants from biomass burning relevant to air quality and human health; however, biomass burning emissions inventories are vital for calculating the impact of fire on atmospheric carbon and climate, but are not covered in this chapter.

The general approach to an emissions inventory for any pollution source is a product of two factors: activity and emission factor (EF) (IPCC, 2007). Activity is defined as the amount of fuel consumption, and the EF converts consumption into emissions. Mass of emissions of a given gas or PM category, M_x (g), is determined with:

$$M_x = M_c \times EF_x, \tag{5.1}$$

where M_c is the mass of fuel consumed (kg) and EF_x (g kg^{-1}) is the emissions factor in mass of gas or PM (x) emitted per mass of fuel consumed (IPCC, 2007; Urbanski, 2014).

Emissions from fuels that burn under controlled conditions, such as gasoline in an internal combustion engine, are well characterized via controlled laboratory experiments. In this case, fuels are standardized and EFs are consistent for a given fuel type, making fuel consumption (activity, in the general context of emissions inventory) the primary variable responsible for determining source emissions strength (the amount of emissions from a source or event). EFs for biomass burning are more varied and complex due to the variety of fuel and combustion conditions possible in open burning. They have been determined through both controlled combustion laboratory measurements and field-based measurements from hundreds of fuel types and various burning conditions. Compilation of EFs for biomass fuels by Prichard et al. (2020) includes more than 12,000 records on 267 air pollutants defined for various fuel types, burn types, locations, and combustion phase (flaming or smoldering combustion).

In the case of biomass burning, in general, the amount of area burned dictates the amount of fuel consumed and is the primary driver of biomass burning emissions magnitude; more burned area means more emissions, with some important qualifiers. Specific attention to the fuel type, density, structure, size, and condition, as well as combustion phase provides more refined estimates of emissions from landscape fire than can be achieved by tallying the area burned alone (French et al., 2002; Prichard et al., 2020). This is because emission contributions greatly differ between different vegetation types (e.g., forest, shrublands, or grasslands) and fuel components, which include aboveground components of tree foliage, fine branches, and shrubs; fine woody fuels (live or dead) and coarse woody debris (decay status); and surface organic material (litter and duff) that compose the fuelbed (see Chapter 4). The relative contributions of these different materials vary greatly within and between wildland fuelbed types, introducing great complexity that drives both fire behavior and fire emissions.

At the same time, the fire environment introduces complexity. Variability in space and time in solar insolation, precipitation, humidity, and other weather variables in the weeks to days prior to the event will influence fuel moisture. Fuel moisture can influence combustion type, namely the flaming and smoldering phases of a fire, which dictates the type of emissions based on combustion efficiency. Combustion efficiency is a measure of how much energy results from a given amount of fuel, with higher combustion efficiency resulting in more complete burning of fuels than low-efficiency combustion. For biomass burning, combustion efficiency is defined as the amount of excess in CO_2 in comparison to total emitted carbon (Yokelson et al., 1999). The fire environment before and during the event, therefore, is an important factor in determining biomass burning emissions across space and time.

Biomass burning emissions inventory and mapping is required as a primary input to smoke concentration mapping, numerical smoke prediction, coupled fire weather-smoke models, and air quality models, as described in Chapters 7, 8, and 9. In this chapter, we review methods to model biomass burning emissions by explaining approaches used to determine fuel consumption and the uncertainties associated with consumption estimates. In section 5.2, we present a general overview of emission factors used in biomass burning emissions inventories, as well as the concept of combustion efficiency, both of which are more completely reviewed in the literature (Prichard et al., 2020; Urbanski, 2014; Urbanski et al., 2021). Approaches to map the location, strength, and composition of fire emissions, considering needs for both retrospective and real-time smoke modeling and forecasting, are considered in section 5.3. Retrospective mapping of emissions has value for greenhouse-gas and aerosol emissions assessments for carbon accounting and climate change modeling as well as for comparing to health outcomes from smoke pollution exposure, which is reviewed later in this book (Chapters 12 and 13). Real-time emissions inventories are used in forecasting potential smoke concentrations downwind from an event (Chapters 7, 8, and 9) or for taking action to avoid exposure (Chapter 10). Finally, in section 5.4, new approaches under development using remote sensing observations for improving estimates of fuel consumption and biomass burning emissions are discussed.

5.2. MODELING BIOMASS BURNING EMISSIONS

Emissions from a fire event are calculated (equation 5.1) from the total fuel consumption for an event (activity, in the general context of emissions inventory) and emission factors (EF) for combustion products for the variety of fuels and conditions found on the landscape. Determination of both fuel consumption and emission factors in the case of biomass burning must take into consideration many factors. The characteristics of the fuels and the conditions of the burn are very important in determining both the amount of fuel consumption achieved during the burning and combustion efficiency, which drives EF. Fuel consumption is determined in various ways in emissions inventory approaches. Two general approaches for determining biomass consumption for wildland fire are presented here followed by a section reviewing the role of emissions factors and combustion efficiency in determining biomass burning emissions.

5.2.1. Fuel Consumption

Conceptually, the most straightforward method to estimate consumption is to difference estimates of the pre- and post-fire fuel loading (biomass density) measured on the ground. At the scale of fire events, maps of pre- and post-fire fuel loading can be derived from pre- and post-fire remotely sensed data trained from field plot data. McCarley et al. (2020) differenced pre- and post-fire fuel maps derived from pre- and post-fire lidar collections to map consumption estimates. Michalek et al. (2000) employed 30 m resolution Landsat data to extend field-measured consumption across a burn site, stratified by fuel type. However, data available from measurement of field-derived consumption are limited due to the onerous task of collecting sufficient quantitative field data to represent the area of interest. Because of this limitation, a field measurement approach cannot be accomplished for quantifying emissions on anything but a local scale.

For comprehensive estimation and mapping of fuel consumption (M_c) two general approaches are commonly used (Wooster et al., 2013; Fig. 5.1). Either of these methods provide the estimate for M_c in equation 5.1 to derive pollutant emissions. The indirect model-based approach uses an estimate of consumption based on the difference between pre- and post-fire fuel loading estimates (McCarley et al., 2020; Ottmar, 2014); alternatively, it can be modeled by multiplying the pre-fire fuel load by a burning efficiency factor. The direct approach estimates consumption based on fire radiative power (FRP) observations, which integrated over time provide an estimate of fire radiative energy (FRE) (Wooster et al., 2005). The terms *indirect* and *direct* refer to how field or remotely sensed observations relate temporally to combustion as a biophysical process, with the indirect approach made from a post-fire assessment, and the direct approach conducted at the time of the event based on active fire data; both approaches can be applied at multiple spatial scales. By the indirect approach, fuel consumption can be estimated at the small scale of paired pre- and post-fire field plots, either destructively from harvest samples (Ottmar, 2014) or remotely from pre- and post-fire terrestrial lidar (Hudak et al., 2020), at the landscape level of an entire fire event from airborne lidar collected pre- and post-fire (McCarley et al., 2020), and at regional-global scales from satellite image passes acquired before and after the burn (Pettinari & Chuvieco, 2016; Rollins, 2009). If post-fire fuel load estimates are unavailable, as is often the case, then a burning efficiency factor (fraction of fuel consumed) can be applied to the pre-fire fuel load estimate to derive consumption. However, it is not possible to directly observe fuel mass loss as it occurs by combustion during a fire event. On the other hand, consumption can be estimated from FRP observations, which provides a suitable surrogate for combustion as it occurs (Wooster et al., 2013). Moreover, FRP and FRE metrics scale readily between ground radiometers and airborne and satellite thermal imaging (Dickinson et al., 2016), making the direct approach a powerful method for near-real-time fuel consumption estimation. These two general approaches are used in the variety of emissions inventory systems described later in this chapter and in Chapter 9.

5.2.2. Mapping Consumption: The Indirect Approach

The indirect approach to mapping consumption is a model-based framework employing generalized information on pre-fire fuel characteristics and the level of consumption based on fuel conditions (French et al., 2014; Ottmar, 2014). Consumption is a product of the

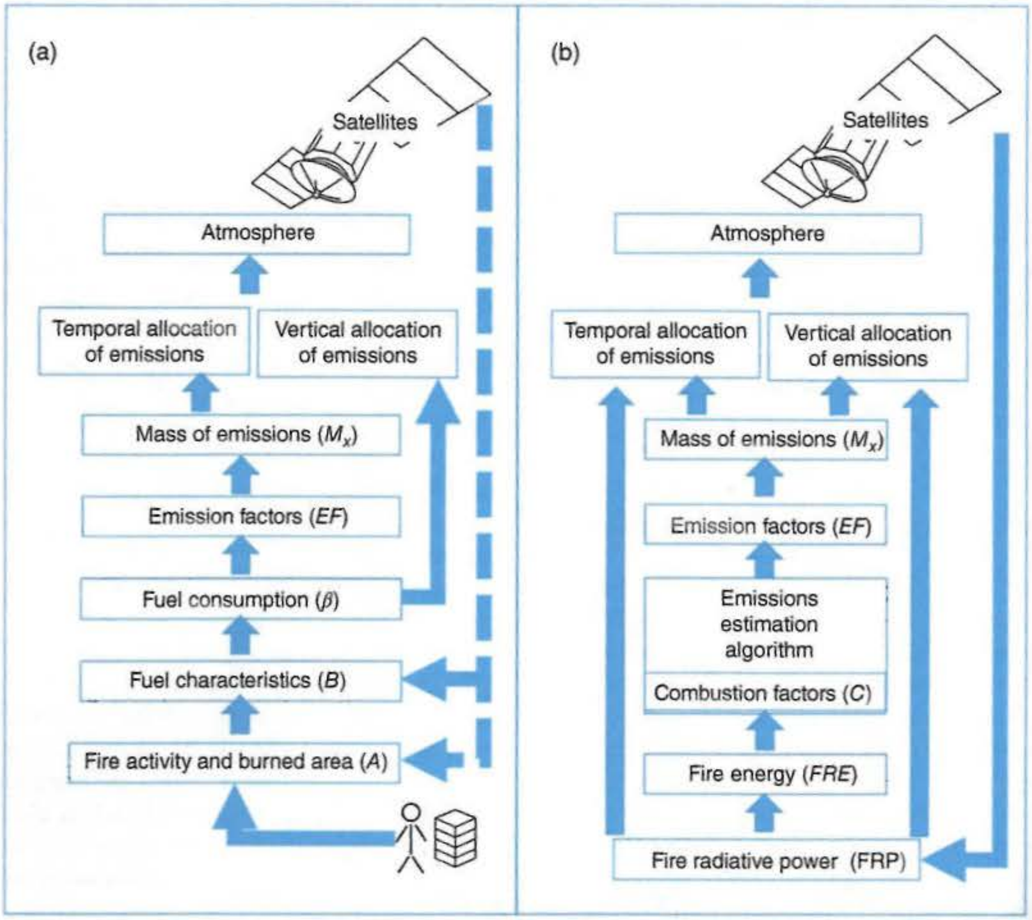

Figure 5.1 Two approaches to determine emissions from biomass burning. Fuel consumption is determined via two methods: (a) The indirect combustion approach considers the pre-fire fuels and proportion of fuel consumed (β). (b) The direct approach uses fire radiative energy to estimate consumption based on fuel-type specific combustion factors (C). Emissions factor (EF) for each product is applied based on combustion conditions. Various methods are used to allocate emissions temporally and vertically for use in atmospheric smoke modeling (see Chapters 8 and 9) (figure courtesy of S. O'Neill).

burn area, the amount of biomass in that area, and the fraction of the biomass consumed (Fig. 5.1), which is also termed *burning efficiency* or *combustion completeness* (van der Werf et al., 2006). The fraction consumed can be defined as a function of several variables, including the moisture conditions of the fuel and combustion conditions in the fire environment. Seiler and Crutzen (1980) used this general framework to make the first global estimates of contemporary carbon emissions from biomass burning, separately considering variation in each term for different biomes and different types of land management. Using this approach, the mass of total fuel consumption (M_c, kg) for an event is calculated using the following general equation:

$$M_c = A \times B \times \beta, \tag{5.2}$$

where A is area burned (m^2) in an event or region, B is biomass density (fuel loading per unit area; kg m^{-2}), and β is the fraction of biomass consumed (0–1, unitless), also termed the *burning efficiency factor*. Circling back to equation 5.1, applying an emissions factor, EF_x, provides the mass of emissions M_x for fuel type x:

$$M_x = A \times B \times \beta \times EF_x. \tag{5.3}$$

Quantification of each of these terms is described in detail next. This general approach has been established as a standard method for fuel consumption from biomass burning. For carbon emissions, the fraction of fuels that is carbon is included as a carbon emission factor, typically 0.45 or 0.5, the nominal carbon content of biomass. For pollutant emissions, used in atmospheric chemistry and air quality modeling, emission factors are applied as shown in equation 5.1 and further discussed later in this chapter.

Active Fire and Burn Area Mapping

In Chapter 2, the drivers of fire occurrence are reviewed explaining that some biomes are naturally fire prone, while other regions have little to no natural fire, and still others are influenced by anthropogenic burning for land clearing and other land use needs (Bowman et al., 2009). The amount of biomass burning varies greatly from region to region and, in some fire-prone ecosystems, from year to year. Determining where and when fire is occurring and the amount of area burned has been a major focus for mapping and monitoring air quality because the magnitude of burning (the amount of burn area (A)) is the dominant factor in many regions driving interannual variability in smoke (van der Werf et al., 2006). Prior to the 1990s, the magnitude of global biomass burning was not well known (Levine, 1991), and there were wide discrepancies in estimates of global fires occurrence (Kasischke & Penner, 2004). The advent of satellite sensing has provided comprehensive observations to better quantify fire occurrence with thermal sensing (Giglio et al., 2003; Kaufman et al., 1998). Multispectral sensing has advanced for mapping land change and burn area products at landscape scales with Landsat (Hawbaker et al., 2020; Key & Benson, 2006) and at regional to global scales with MODIS and similar systems (Giglio et al., 2006). Estimates of biomass burning (burn area and fire counts) for various regions of the world are fairly well constrained due to the advent of satellite-based systems for fire monitoring (Chapters 2 and 3).

For some regions and fuel types, accurate accounting of biomass burning is challenging. Satellite-based methods for determining burn area suffer from a mismatch in resolution between the sensor and the phenomenon; where fire is typically confined to a narrow fire-line of meters to submeter scale, satellite sensors detect energy at several meters to kilometer scale. This requires methods to subsample the information, often leading to bias of too much area burned (Hyer & Reid, 2009). On the other hand, satellite sensors also suffer from characteristics leading to undercounting of burn area by missing fires due to both the sampling rate of the orbiting satellite sensor and the obscuration of the fires under tree canopies or cloudy skies (Cochrane et al., 1999; Johnston et al., 2018; Morton et al., 2011; Souza et al., 2005). Agricultural burning and other small fires, such as pile burning practices, are missed in many emissions inventories for these reasons (Randerson et al., 2012). In addition, smoldering fires that are known to last for weeks to months, and can even reignite after winter hiatus, can consume large areas of organic peat soils, emissions that are undeniably undercounted (McCarty et al., 2021).

Figure 5.2 provides an example of a case in the southeastern United States where prescribed fires are common. The extensive omission errors are caused by the 16 day overpass frequency of the Landsat satellite, coupled with occlusion from cloud cover. Moreover, most fires in the ecosystems at both locations are low-intensity prescribed surface fires burning beneath the tree canopy; hence, canopy occlusion causes further underestimation of the true burn area, as recorded on the ground, causing some fires to be entirely missed (shown as empty blue polygons). In this case, satellite-based accounting misses 80% of the actual area burned recorded from fire records. This is a common problem in accounting for fire in any forests that have dense canopies and support understory burning, including tropical forests, which are typically low-intensity understory fires where dense forest canopies and clouds are common (Morton et al., 2013). Methods that use pre- and post-burn images for mapping burn area, and do not rely on active fire, are employed (Hawbaker et al., 2020); however most burn area products are seeded with locations mapped from active fire sensing (Giglio et al., 2006), because detection of burn locations in some biomes and ecosystems can be subtle, resulting in missed fires. Chapter 3 reviews these and other caveats in relying on satellite data alone for emissions inventory.

Because satellite remote sensing cannot capture all burning relevant to air quality, approaches that include record-keeping techniques are often required. Within the United States, the USEPA relies on a data consolidation effort that combines fire records with satellite detections (SmartFire-2) (Larkin et al., 2020) to account for fire in the triennial National Emissions Inventory (NEI). Therefore, the United States and other national fire activity assessments for emissions reporting rely heavily on satellite-based active fire and burn area data, as reviewed later in this chapter and in Chapter 9. In general, fire accounting will always miss some fires and area burned, as has been documented by Hall et al. (2016).

Biomass and Fraction Consumed

Estimating the amount of consumption within the perimeter of a burn based on the model shown in equation 5.2 can be highly uncertain due to the high variability in both the amount of fuel (loading) at the site (B) and the fraction consumed (β) (French et al., 2002, 2004; Urbanski et al., 2011; van Leeuwen et al., 2014). To estimate emissions where no pre- or post-fire fuel loading measurements are available, consumption must be modeled based on field data that relates consumption to measurable variables (fuel characteristics and moisture status). Examples of consumption models are the Consume model (Prichard et al., 2006), the First Order

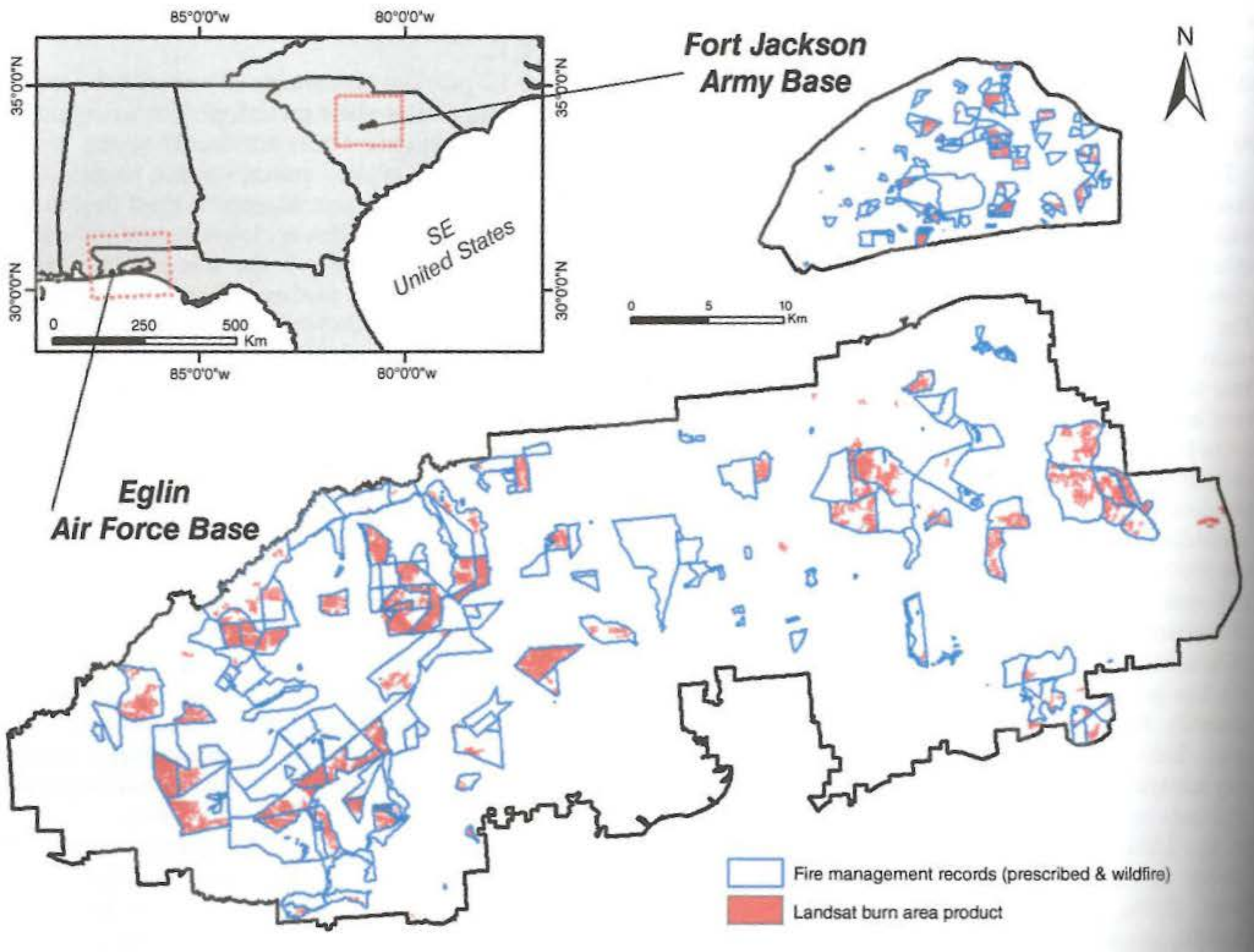

Figure 5.2 Fire management records of 2014 prescribed and unintentional fire perimeters versus remote sensing-derived burn area from the Landsat burn area product (Hawbaker et al., 2020) at Ft. Jackson Army Base and Eglin Air Force Base, located in the southeastern United States, showing extensive omission errors from canopy and cloud obscuration and low satellite repeat frequency (figure courtesy Dr. Nuria Sanchez-Lopez).

Fire Effects (FOFEM) model (Reinhardt et al., 1997), and CanFIRE (de Groot et al., 2009), which are used as the basis of several emissions model systems. All of these models rely on knowledge of the fire environment, including the pre-fire fuels and the fuel moisture, which are a function of weather and climate.

Pre-fire fuel loadings can be estimated from remotely sensed data, typically multispectral (e.g., Landsat) satellite imagery, trained from field plot measures. National LANDFIRE maps are the best example in the United States (Rollins, 2009). The Fuel Characteristics Classification System (FCCS) developed by Ottmar et al. (2007) provides a comprehensive framework for summarizing complex fuelbeds into their component materials (trees, shrubs, herbaceous, coarse and fine woody debris fractions, litter, duff); the proportions of these components vary greatly by vegetation type. Landsat imagery FCCS fuelbeds have been mapped for the United States based on LANDFIRE Existing Vegetation Type (EVT) maps (Rollins, 2009). Globally, FCCS has been mapped from MODIS-derived vegetation type for use in fire emissions modeling in many regions around the world, including South America (Pettinari et al., 2013), and as a global product (Pettinari & Chuvieco, 2016). The original purpose of developing the FCCS was for fire planning and management to provide fire managers with site-level fuel information from which they could estimate fire behavior (e.g., spread rate), consumption, emissions, and fire effects for a given set of fire weather and fuel moisture conditions. The Consume and FOFEM models were developed to use FCCS fuels for site-level consumption estimation but have been used with LANDFIRE FCCS layers to increase their applicability at broad scales (French et al., 2014) and in smoke model environments (e.g., BlueSky Tools; Larkin & O'Neill, 2018; Larkin et al., 2009; see Chapter 9).

Weather and climate factors that influence fuel consumption are best considered as a continuum of constraints on combustion, operating at different temporal scales. Fire weather variables (wind, temperature, and RH) have the most immediate effects, operating at seconds to days, while climate variables, such as growing season length, operate at seasonal to decadal time scales. In the absence of fire, climate operates to constrain vegetation production, senescence, and mortality, and thereby fuel loads, as a balance between accumulation and decomposition (Olson, 1963). Occupying the middle ground between weather and climate at an intermediate temporal scale, ranging from hourly to seasonally, is fuel moisture, constrained by the full continuum of weather-climate factors and landscape physiography. These factors include temperature, precipitation, evapotranspiration, relative humidity, wind, slope, aspect, and soil type. Fuel moisture is a critical control on combustion and is difficult to monitor remotely (Chowdhury & Hassan, 2015; Yebra et al., 2013) given that it is temporally very dynamic for each fuel component, depending on particle size and arrangement (see Chapter 4) (Viegas et al., 1992; Viney, 1991). Despite this complexity, moisture status of dead fuels is easier to parameterize in fuel moisture models by fuel size class than live fuel moisture content (Carlson et al., 2007; Finney, 1998; Nelson, 2000, 2001), because plants in their various functional forms exhibit a variety of strategies in response to water limitation and drought (Viegas et al., 2001). However, fuel moisture is the basis of fuel consumption models, providing the most important constraint on combustion, making it a very important variable in emissions estimation, no matter the approach used.

5.2.3. Mapping Consumption: The Direct Approach

Active fire sensing can provide a direct estimate of biomass consumption derived from the energy emitted (Wooster et al., 2003), unlike the indirect approach, which determines consumption from a model-based accounting of fuel consumption (Fig. 5.1). Fire radiative power (FRP) observations are derived from calibrated brightness temperatures measured by thermal infrared imaging sensors (Dozier, 1981; Kaufman et al., 1998). Fire radiative energy (FRE) is the time integral of instantaneous FRP observations, expressed as follows:

$$FRE = \int_{t1}^{t2} FRP(t)\,dt. \tag{5.4}$$

This integral can be approximated by the following equation (Boschetti & Roy, 2009; Hudak et al., 2015):

$$FRE = \sum_{i}^{n} 0.5\left(FRP_i + FRP_{i-1}\right)\left(t_i - t_{i-1}\right), \tag{5.5}$$

where time t is the time in seconds (s) of each FRP observation, i, in the time series.

FRP and FRE are extremely useful because they are linearly related to combustion rate and total consumption, respectively (Wooster et al., 2005). The direct approach to estimating the consumption mass, M_c, is as follows (Prichard et al., 2021; Wooster et al., 2013):

$$M_c = FRE \times C, \tag{5.6}$$

where C is a combustion factor (kg MJ^{-1}) for a given vegetation (fuel) type, which equates to the slope of the linear best fit relationship between and FRE and the mass of fuel consumed, M_c (Wooster et al., 2013). An advantage of the direct approach to consumption estimation by equation 5.6 is that it replaces the burn area, biomass, and fraction consumed variables in equation 5.2. Thus, the combustion factor C (kg MJ^{-1}) converts energy units (MJ) to mass units (kg) of fuel consumed (M_c) to effectively collapse the three predictors used in the indirect approach of equation 5.2 into a single coefficient. The combustion factor varies considerably as a function of fuel moisture (Smith et al., 2013). Circling back to equation 5.1, applying EF_x provides the mass of emissions M_x for fuel type x:

$$M_x = FRE \times C \times EF_x. \tag{5.7}$$

Inherent underestimation biases confound FRE-based consumption estimation from remote sensing observations. The origin of these biases parallel those for estimating consumption in the indirect method. They include obscuration from clouds, smoke, and tree canopies and limitations in observation due to satellite orbit characteristics. Mathews et al. (2016) found that forest with complete or nearly complete canopy closure can obscure fire and may be below the detection threshold of above-canopy FRP sensors. Global satellite FRP products are derived from polar-orbiting satellites (e.g., MODIS) that image a given location on the Earth twice daily at most, assuming no cloud cover (Roberts et al., 2011); this translates into many missed ignitions and unobserved flame front movement between satellite overpasses and where clouds are present during the overpass. At the regional scale of northern Australia, which has a very active fire regime, Boschetti and Roy (2009) used simple kriging to spatially extrapolate sparse MODIS observations of FRP using the independently derived MODIS burn area product, to derive FRE estimates that were less affected by undersampling. Similarly, at the landscape scale of individual prescribed fires, Klauberg et al. (2018) used ordinary kriging and conditional simulation to extrapolate FRE estimates integrated from temporally undersampled FRP observations collected from an infrared camera mounted on a fixed-wing aircraft flying laps over the fire. In both of these examples, geostatistical modeling (e.g., kriging) served to fill in the spatial gaps caused by undetected burning between the sparse fire observations.

5.2.4. Addressing Complexity in Fuels and Combustion

As described in Chapter 4, biomass fuels are heterogeneous in characteristics relevant to emissions. Even in areas of monoculture forests or grasslands, topographic and hydrologic features can influence the fuel conditions and drive variability in combustion. Fuel components, meaning the fuel type and vegetation strata (see Chapter 4), have very different burning properties, making assignment of combustion factors by vegetation type a gross oversimplification, especially for global-scale assessment when generalized vegetation type is often used in this way (e.g., land cover class or biome; Kaiser et al., 2012; van der Werf et al., 2006; Wiedinmyer et al., 2011).

One strategy for addressing fuel complexity for more accurate consumption estimates via the indirect method is by modeling combustion by fuel component or strata, for example assigning different β values in equation 5.2 to the aboveground and surface fuels (French et al., 2002). In this example, equation 5.2 is expanded to include two fuel components as:

$$M_x = A \times \sum B_a \beta_a + B_s \beta_s, \tag{5.8}$$

where B_a is the average biomass density of aboveground vegetation and B_s is the loading of the surface fuels, with corresponding consumption fractions β, for each stratum. This can be applied to more than two fuel components or strata, and is one of the strategies used in several consumption approaches, including the Global Fire Emissions Database (GFED) (van der Werf et al., 2017; van Leeuwen et al., 2014) and the Consume model, which uses the FCCS fuelbed paradigm (Ottmar, 2014). In addition, separating combustion models by fuel component allows for explicitly defining combustion phase for assigning emission factors, thereby improving the estimate of emissions of non-CO_2 gases by accounting for combustion efficiency (see section 5.2.5).

5.2.5. Emission Factors and Combustion Efficiency

Smoke from biomass burning is a complex mixture of gases and particulate matter (PM) (Table 5.1; Prichard et al., 2020; Urbanski, 2014). The most abundant gases in smoke from fires burning wood and other biomass are carbon dioxide (CO_2), carbon monoxide (CO), methane (CH_4), nitrogen oxides (NO, NO_2), ammonia (NH_3), and sulfur dioxide (SO_2) (USEPA, 2021a). Nitrogen oxides, grouped together as NO_x, are especially important for their role in the formation of ozone (O_3) through a photochemical process, which is a critical pollutant in downwind smoke. Important for air quality, nonmethane hydrocarbons, organic aerosols, and other organic and inorganic pollutant compounds are found in smaller but sometimes critical levels in smoke, most often in incomplete combustion conditions (Andreae & Merlet, 2001). PM in biomass burning smoke is a mixture of fine to very fine solid particles and liquid droplets. Alternative terminologies for PM are *total particulate matter (TPM)* or *total suspended particles (TSP)*. Particulates that are lofted into the air form aerosols, a collection of suspended particles of varying composition, shapes, and sizes. PM is often designated by size; typical designations are particles

Table 5.1 Emission Factors (EF) for the primary pollutants in biomass burning smoke

	Mean (SD) of all data in SERA	Mean (SD) by combustion phase	
Pollutant	Emission factor (EF) (g/kg)	EF flaming (g/kg)	EF smoldering (g/kg)
Carbon dioxide CO_2	1,595.6 (166.2)	1,671.4 (78.2)	1,521.2 (148.5)
Carbon monoxide CO	99.042 (49.430)	70.363 (22.700)	131.593 (40.013)
Particulate matter <2.5mm - $PM_{2.5}$	22.456 (16.954)	15.957 (9.884)	31.804 (18.880)
Methane CH_4	4.294 (3.387)	2.618 (1.345)	7.628 (3.338)
Nitrogen oxides NO_x	3.021 (2.110)	2.755 (1.143)	2.288 (2.016)
Ammonia NH_3	1.386 (1.445)	0.889 (0.768)	2.576 (1.886)
Sulfur dioxide SO_2	1.113 (0.723)	1.025 (0.552)	1.569 (1.158)

Source: This information is compiled and condensed from the Smoke Emissions Reference Application (SERA), Prichard et al. (2020).

Note: Units are in g of a gas or PM per kg of fuel consumed (Mc). Also shown are EFs for flaming and smoldering combustion conditions. Standard deviation (SD) of measurement mean is shown in parentheses. The number of data samples varies. We are considering fire in areas with few to no houses or human-built infrastructure. Smoke from fires that consume structures contain a myriad of additional compounds, which will not be reviewed in this chapter.

with a diameter <2.5 μm ($PM_{2.5}$) and particles with a diameter <10 μm (PM_{10}), which include the smaller category of particles. Smaller particles ($PM_{2.5}$) are more influential on human health and often the subject of health studies because they can be respired deeper into the lungs than coarse particulates (see Chapter 11). Additionally, these small particles stay aloft longer, so can be transported farther, causing impacts to air quality far from the site of the event (Seinfeld & Pandis, 1998).

Emission Factors

For all sources, emission factors (EFs) define the partitioning of combustion products into various emission products and are variable based on the fuel type and combustion conditions. Biomass burning, EFs are determined by measuring the concentration of a pollutant either in the lab or in a field-measured fresh smoke plume against a background concentration (Urbanski et al., 2021). Seasonal and regional variability in EFs is well known. For global scasle emissions inventories, specific EFs are applied by biome (Kaiser et al., 2012; van Leeuwen et al., 2013). For event-based and regional efforts, EFs are on the fuel type and combustion conditions (Prichard et al., 2020). Studies of African savannah grasslands identified some of the underlying factors driving variability in these ecosystems (Hoffa et al., 1999; Korontzi, 2005); these and similar studies provide some guidance for improving EFs used in biomass burning emissions modeling. Regionally defined variability in biomass burning CO emissions and concentrations using six EF scenarios was assessed in a study by van Leeuwen (2014). The study used both spatial variability defined by biome and temporal variability, as opposed to previous approaches that employed static EFs by biome (Akagi et al., 2011). Using this spatial-temporal complexity in EF, van Leeuwen (2014) found an increase in CO emissions for boreal regions (as much as 50%), but lower estimates for Africa (~3.5%), compared with using static EF values, revealing the importance of refined knowledge of EF over space and time for accurate emissions and smoke concentration mapping.

Recent efforts to better characterize the composition of smoke for emissions modeling have resulted in several updates to EFs from biomass burning and other open burning (Akagi et al., 2011; Andreae, 2019) and include the development of the Smoke Emissions Repository Application (SERA) database of biomass burning EFs for smoke modeling (Prichard et al., 2020). SERA lists over 275 species of gases and particulate categories; the primary gases and aerosols and an average EF as reported in SERA are listed in Table 5.1. A subset of the pollutant list in SERA is the criteria air pollutants (CAP) designated by the USEPA. It should be noted that one of the primary pollutants of interest for air quality assessment, ozone (O_3), is not included in this table because it is not a primary product of combustion, rather is formed when nitrous oxides (NO_x) in smoke interact with sunlight through photochemistry. Similarly, aerosols are known to evolve as they age (Huang et al., 2013; Kleinman et al., 2020), so typically EFs are reported from fresh smoke, unless otherwise noted.

Combustion Efficiency and Emissions

Variations in emissions and EFs are driven by various compounds in the biomass as well as the combustion conditions. Combustion type or combustion phase is determined by the conditions under which the combustion process occurs, which is a result of fuel water content, fuel compaction, and ventilation (wind), all of which influence available oxygen. Low oxygen conditions during a smoldering burn produces a very different set of combustion products than clean burning, where oxygen is not restricted, as shown in the EF differences due to combustion phase (Table 5.1). Smoldering conditions reduce the combustion efficiency thereby decreasing the amount of CO_2 at the same time as increasing the formation of CO and gaseous and particulate organic compounds that can have high toxicity, so are therefore of concern for human health (Rappold et al., 2011; see Chapter 11).

Modified combustion efficiency (MCE) is a way to quantify the level of inefficient combustion found especially during the smoldering phase. MCE is calculated from the concentrations of CO_2 and CO in the plume compared to the nonplume (background) concentration, as shown in Eq. 5.9 with Δ indicating plume to background difference (Yokelson et al., 1999):

$$\mathrm{MCE} = \Delta CO_2 / \left(\Delta CO_2 + \Delta CO\right). \qquad (5.9)$$

Efficient combustion will have an MCE of 1 indicating that all carbon in the fuel is emitted as CO_2. The MCE indicates the relative amount of flaming and smoldering combustion, with a lower MCE indicating more smoldering. Typical MCE values for wildfire biomass combustion are 0.80 to 0.95. MCE measured in smoke provides a way of defining the relative amount of complex combustion products, such as organic gases and aerosols, critical to air quality. As reviewed in Urbanski et al. (2021), MCE tends to differ with fuel type, with MCE highest for herbaceous (grass and forb) and shrub-type fuels and lower for forest fires (Fig. 5.3). In general, MCEs for prescribed fire tend to be higher than for wildfires, indicating cleaner burning in prescribed versus wildfire, although this generalization is broad, and MCE is highly variable in all open burning situations (Prichard et al., 2020).

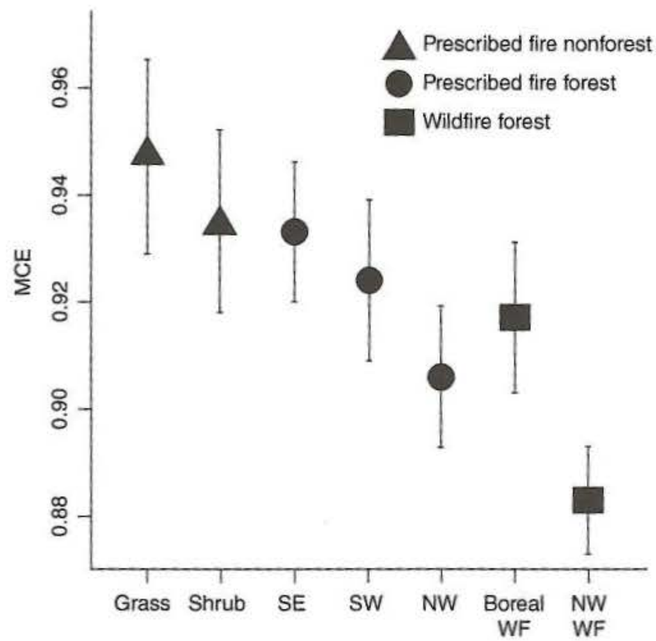

Figure 5.3 Figure demonstrating the variation possible of modified combustion efficiency (MCE) for fire in different vegetation types and biomes of the United States (US). SE = southeast US, SW = southwest US, NW = northwest US, and WF = wildfire. Error bars are 1 standard deviation of the measured data (reproduced from Fig. 6 in Urbanski, 2014).

5.3. BIOMASS BURNING EMISSIONS INVENTORIES AND MAPPING SYSTEMS AND PRODUCTS

The variety of emissions inventory approaches has resulted in disparate estimates of the impacts of fires on pollutant concentrations. Emissions estimates of some chemical species may vary by a factor of 3 to 4 (Urbanski et al., 2011). In this section, we review existing models, systems, and products for emissions inventory and mapping, including approaches used for national fire emissions inventories and modeling systems used for event-scale assessment of smoke plumes to global-scale understanding of atmospheric chemistry. Chapter 9 provides a more specific review of air quality models from several nations that use the methods described in this chapter.

5.3.1. National-Level Emissions Inventories

Monitoring air pollution on a global scale is challenging, requiring multiple governmental and quasi-governmental efforts to bring the science of emissions monitoring to the task (Frost et al., 2013). The work to quantify pollutants has primarily been carried out to inform in-country and transboundary regulatory requirements. The Convention on Long-Range Transboundary Air Pollution (LRTAP) was set up in 1979 by 51 nations to address transboundary air pollution. LRTAP provides a framework for monitoring specific pollutants to address transboundary air pollution in North America, Europe, and Russia and former East Bloc countries (UNECE, 1979). In a separate effort, much of the work on quantifying emissions from biomass burning has been carried out for purposes of climate change monitoring, which is concerned with CO_2 and other climate-relevant gases and aerosols, also called greenhouse gases (GHG). Often GHG assessments present results in total carbon emissions or CO_2 equivalents, rather than for toxic air pollutants that are of concern for human health studies. The initiative to quantify GHG emissions from biomass burning has provided a framework to account for and quantify pollutant source emissions using methods prescribed by the IPCC (2007). Recent efforts to reconcile the different approaches for multiple needs of climate and air quality have provided guidance for including biomass burning in national-scale emissions inventories (Vallack & Rypdal, 2019).

National governments around the world conduct inventories of air pollutants and GHG emissions from biomass burning and other open burning. As an example, the U.S. National Emissions Inventory (NEI) compiles detailed estimates of air pollutants and precursors every 3 yr from state and regional government agencies, reported by county or state, depending on the data source. In addition to general air pollution sources, such as vehicles and power plants, the NEI accounts for fire and agricultural burning with extensive improvements to methods beginning in the 2011 NEI (Fig. 5.4) (Larkin et al., 2020). In a separate effort for climate assessment purposes, the *Inventory of U.S. Greenhouse Gas Emissions and Sinks* (USEPA, 2021b) has been compiled annually since the early 1990s; it is submitted to the United Nations in accordance with the Framework Convention on Climate Change (UNFCCC) reporting requirements (UNFCCC, 2021). Similarly, in the European Union, the European Monitoring and Evaluation Programme (EMEP) started publishing a guidebook on air pollutant emissions in 1992 and it has been maintained under the LRTAP Convention. The guidebook includes emissions sources from forest and grassland fires, as well as agricultural burning and continues to be published by the European Environment Agency (EEA), most recently released in 2019 (European Environment Agency, 2019). Canada and Australia have extensive areas of burning that vary annually. They both conduct detailed accounting of emissions from fire in their annual GHG reports to the UNFCCC using IPCC reporting methodologies, and both have national air quality monitoring programs akin

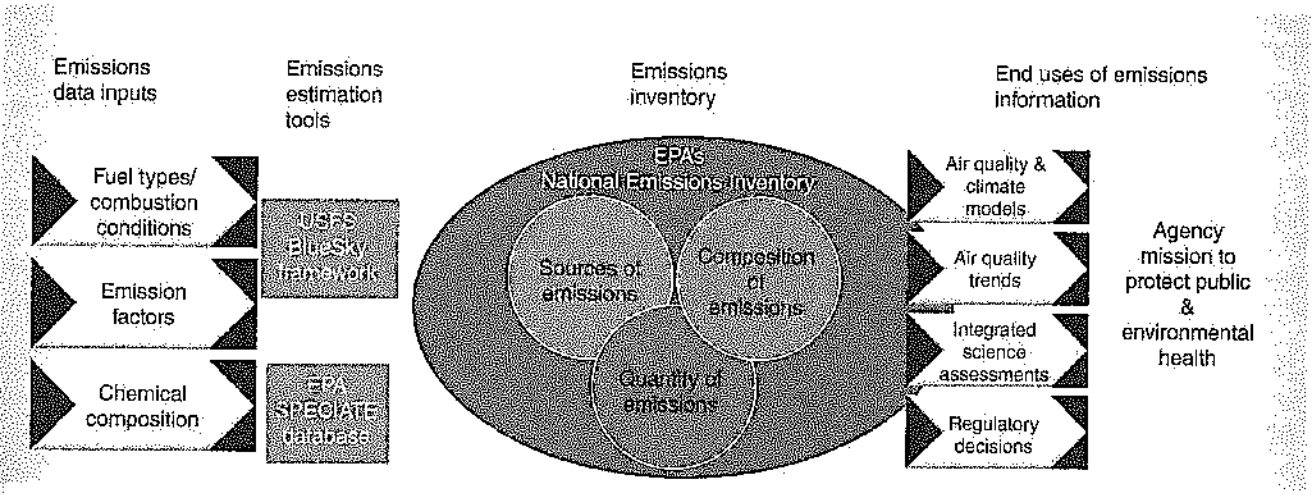

Figure 5.4 Overview of the U.S. Environmental Protection Agency approach to wildland fire emissions inventory. For more information see Holder (2019).

to the U.S. EPA and E.U. EMAP programs. Additional information on country-level efforts to model and track pollution from fire is provided in Chapter 9.

5.3.2. Fire Emissions Inventory Systems

Outside of needs for national and international reporting and regulatory compliance, fire emissions are tracked for a variety of needs and stakeholders. Table 5.2 provides a list of some of the emissions monitoring and inventory systems currently in use. Many of these efforts are focused on GHG emissions tracking, with some having been adopted for integration into air quality models. Global-scale emissions inventory approaches are available for retrospective emissions inventory, such as the Global Fire Emissions Database (GFED) and for direct use in atmospheric chemistry modeling and forecasting (see Chapter 9). Global-scale models provide a comprehensive method to understand fire in the Earth system, and can allow for more complete and accurate modeling of atmospheric processes. The different approaches used incur tradeoffs and assumptions to achieve the goals of the assessment. The Global Fire Assimilation System (GFAS; Kaiser et al., 2012), the NASA Fire Energetics and Emissions Research (FEER) algorithm (Ichoku & Ellison, 2014), and the global biomass burning emission product from geostationary satellites (GBBEP-Geo; Zhang et al., 2019) use the fire energy approach (FRE) described previously, which employs a combustion factor to relate energy and emissions with broad assumptions regarding EFs for an event as well as fuel type and condition. FINN blends indirect and direct modeling approaches with generalized information on fuels and satellite-derived active fire detections to produce emissions on a daily basis (Wiedinmyer et al., 2011). These systems produce results in near-real-time, meaning the estimates are made as fires occur in order to provide data for numerical weather prediction and atmospheric modeling (see Chapter 9).

Finer-scale emissions inventory approaches are used for mapping smoke from individual fires and regions and to gain more specific and refined estimates of emissions for landscape and regional applications. The USDA Forest Service's Wildland Fire Emissions Inventory (WFEI) (Urbanski et al., 2011) was completed to estimate fine-scale emissions for the western United States from 2003 to 2008 in order to assess the reliability and uncertainty of coarse-scale estimates from other global inventories (see Chapter 9). The Canadian Wildland Fire Information System (CWFIS) provides twice-daily input on fire emissions for Canada's Wildfire Smoke Prediction System (FireWork) daily smoke forecast maps. The underlying emissions model for CWFIS modeling is CanFIRE (de Groot et al., 2009), which is also integrated into the national emissions reporting for GHG. The Wildland Fire Emissions Inventory System (WFEIS; French et al., 2014) operates on historical fire data and was developed to provide a spatial mapping capability to nonspatial emissions modeling using Consume (Prichard et al., 2009). WFEIS uses the indirect method, intersecting fire perimeter location and time-stamp data with fuel information from the FCCS (see Chapter 4) mapped by LANDFIRE (Rollins, 2009), and weather-derived fuel moisture, to make an indirect estimate based on equations 5.1 and 5.2. BlueSky is an emissions modeling and smoke forecasting framework that is used to map

Table 5.2 Fire emissions modeling systems currently available showing temporal and spatial domain

System	Approach	Temporal domain	Spatial domain	Spatial scale	Reference(s); websites
GFAS	Direct	2003 pres; NRT	Global	0.1° of lat/long	Kaiser et al., 2012 https://www.ecmwf.int/en/forecasts/dataset/global-fire-assimilation-system
FEER	Direct	2003 pres; NRT	Global	0.1° of lat/long	Ichoku & Ellison, 2014 https://feer.gsfc.nasa.gov
GBBEPx	Direct	NRT	Global	0.1° of lat/long	Zhang et al., 2019 https://www.ospo.noaa.gov/Products/land/gbbepx
GFEDv4	Indirect	1997–2016	Global	0.25° of lat/long	Giglio et al., 2013; van der Werf et al., 2017 https://www.globalfiredata.org/
FINN	Indirect	2002–2013 NRT	Global	1 km	Wiedinmyer et al., 2011 https://www2.acom.ucar.edu/modeling/finn-fire-inventory-ncar
BlueSky (emissions)	Indirect	NRT	United States	Various	Larkin et al., 2009 https://www.airfire.org/data/bluesky
WFEIS	Indirect	1983–2020	North America	Various	French et al., 2014 https://wfeis.mtri.org

Note: NRT = near real time, indicating estimates are produced as the events happen.

emissions sources in a way that can be ingested into air quality and other smoke transport models (Larkin et al., 2009). The BlueSky emissions model uses similar inputs as WFEIS and uses the Consume model to make an indirect estimate of consumption and emissions. It has been used for the triennial U.S. NEI to estimate source emissions for input into the Community Model for Air Quality (CMAQ; Byun & Schere, 2006). BlueSky is described in detail in Chapter 9. In addition to the models listed in Table 5.2, Chapter 9 provides additional insight into the emissions modeling and inventory data used in operational smoke mapping and forecasting around the world.

5.4. APPROACHES FOR IMPROVING FUEL CONSUMPTION ESTIMATES FOR EMISSIONS INVENTORIES

Existing approaches for quantifying the magnitude and extent of fire emissions across the landscape are inherently limited by lack of knowledge about conditions within and during the fire event. Most emissions inventories rely on generalized maps or unconfirmed knowledge of fuel loadings and structure. Approaches often use rules of thumb regarding combustion conditions and averages of important parameters that define emission magnitude and type. Furthermore, once emissions are calculated, in order to use the information for smoke exposure, they need to be integrated into a smoke transport model to map air quality concentration (see Chapter 8). To integrate emissions with transport models that operate at minute to hour time steps, a temporal profile must be assigned to allocate the daily results to the required time step of the smoke model, introducing another set of assumptions. Because of these various assumptions and the inherent variability in fuels and the fire environment, large differences are found when simulated smoke composition is compared with remote sensing measurements or in situ observations (e.g., Pfister et al., 2011; Yao et al., 2013). Pfister et al. (2011) modeled sources of CO and found high uncertainty and an underestimate of CO from fires when compared with measurements collected during an airborne sampling campaign aimed at quantifying sources of CO over northern California.

The high variability in emissions from biomass burning has ramifications for air quality modeling and forecasting. Attempts at error analysis for emissions have been elusive, mainly due to the lack of measurements to characterize the uncertainty (French et al., 2004). For this reason, techniques to better describe the system with more complete observations are required. In this section we review a few avenues under way to help better describe the state of emission variables, including burn area and consumption. Not included here is a review of recent advances in fuels characterization, burn area mapping and measuring emission factors (EF). Chapter 4 covers advances in fuels characterization relevant for emissions modeling. Burn area improvements are reviewed in Chapter 3. Recent improvements in measuring and quantifying EFs can be found in the literature coming out of the 2018 Western Wildfire Experiment for Cloud Chemistry, Aerosol Absorption and Nitrogen (WE-CAN) (e.g., Selimovic et al., 2019) and the 2019 Fire Influence on Regional to Global Environments and Air Quality (FIREX-AQ) (NOAA, 2021) campaigns, recent intensive studies of North American fire emissions and smoke composition.

5.4.1. Improving Indirect Fuel Consumption Estimations

Estimates of M_c by the indirect approach are highly sensitive to the source of burn area information used (Knorr et al., 2012). Estimates using standard modeling methods (equation 5.2) vary widely, with large uncertainties that are difficult to quantify (Fortin, 2021; French et al., 2004; Urbanski et al., 2011). This inherent variability, and therefore uncertainty, in quantification of fuel consumption is founded in the variability of both the fuel loading (B) and the amount of fuel consumed (β in equation 5.2 and C in equation 5.6). Uncertainties in fuel loading and burn efficiency can exceed 100% (Reid et al., 2009; Wooster et al., 2013), as these predictors are considerably difficult to quantify at any scale (Boschetti & Roy, 2009; French et al., 2004; Schultz et al., 2008; Wooster et al., 2005). It has been empirically demonstrated that fuels in natural fuelbeds fundamentally vary at submeter scales (Keane, 2012, 2015; Keane et al., 2012).

The indirect approach to estimating consumption relies on poorly parameterized empirical models of consumption based on a small sample of consumption measurements by fuel type and strata (e.g., the Consume model; Ottmar, 2014; Prichard et al., 2009). Van Leeuwen et al. (2014) published the first attempt at a comprehensive, global database listing all the available fuel consumption field measurements in the peer-reviewed literature. Estimates range from 4.6 ± 2.2 t ha^{-1} in savannas to 314 ± 196 t ha^{-1} in tropical peat lands, which represents anywhere from 21% to 96% of available fuel consumed, depending on the fuel category and biome (Table 2 in van Leeuwen et al., 2014). Based on van Leeuwen et al. (2014), some biomes and regions are drastically undersampled, including tundra regions, agricultural landscapes, and peat lands. The high level of variability in pre-burn fuel loading (Prichard et al., 2019) and combustion loss makes it very difficult to measure enough samples to fully characterize fuel consumption for this type of model. An improvement would be spatially explicit estimates of consumption that capture fuel heterogeneity, or more samples to inform the empirical models. The challenge is to develop a framework for modeling fuels and fire regimes that accounts for spatiotemporal variability in fuels. This framework will necessarily be informed by both remotely sensed and field measurements collected at multiple spatiotemporal scales. Uncertainties in maps of estimated fuels and consumption are expected to be high at the resolution of pixel-based estimates but improve upon aggregation to entire fire events (Hudak et al., 2015; Klauberg et al., 2018), which is the scale domain of emissions models needed for air quality mapping.

Lidar has been found to be an excellent tool in characterizing forest structure (Wulder et al., 2008), and is now being used experimentally to estimate fuel loading because of its great sensitivity to vegetation structure that correlates to fuel loading (Hudak et al., 2002). Unlike passive optical imagery (e.g., Landsat), which saturates under high biomass conditions, lidar is sensitive to increasing biomass without asymptote (Hudak et al., 2020; Kennedy et al., 2018; Zhang et al., 2014). Airborne lidar collections are becoming widespread, particularly in the United States and particularly in forested lands, where the canopy penetrating capabilities of lidar provide the most accurate ground elevation measurements from which to interpolate a high-resolution (e.g., 1 m) digital terrain models (DTM) from the ground returns. The strategy of the 3D Elevation Program (USGS, 2021) is to collect lidar data wall-to-wall across the coterminous United States within 10 yr, to populate a national elevation data set with unprecedented accuracy and precision at 1 m resolution. Such lidar can also be used to characterize pre-fire fuel loading, providing detailed information not otherwise available in such detail (Popescu et al., 2003; Skowronski et al., 2007). In the case of large wildfires where whole watersheds may be burned, landslides and broad-scale erosion become a critical concern of local watershed managers, especially for municipal water provisions, which has motivated post-fire lidar collections in specific cases to quantify such changes. While relatively rare, these pre- and post-fire lidar collections provide an opportunity to estimate fuel consumption, at unprecedented spatial resolution that no other technology can provide, simply by differencing maps of pre- and post-fire fuel loading, as demonstrated by McCarley et al. (2020). The advent of spaceborne lidar sensors with global coverage (e.g., Global Ecosystem Dynamics Investigation (GEDI); Ice, Cloud, and Land Elevation Satellite (ICESat-2)) provide dramatically expanded monitoring capabilities for estimating consumption using pre- and post-fire lidar. Spaceborne waveform sampling instruments with larger instantaneous coverage (footprint) than typical airborne lidar systems could provide estimates of fuel loading at the footprint level; for

ICESat-2 this is a 25 m diameter footprint, similar in size to a forest inventory plot (Leite et al., 2022). Such estimates can be augmented with pre- and post-fire passive optical imagery (e.g., Sentinel or Landsat) using statistical or geostatistical models (Hudak et al., 2002) to generate pre- and post-fire fuel maps from which to estimate consumption.

5.4.2. Improving the Direct Approach to Fuel Consumption and Emissions Estimation

The biggest contributor to uncertainty in the direct approach to estimating consumption and subsequent emissions, based on FRE, is undersampling of FRP over the course of the fire event. The largest factor contributing to underdetection is the infrequent overpasses of polar orbiting satellites (e.g., twice daily for MODIS) relative to daily active fire at a given location (Boschetti & Roy, 2009). Cloud and smoke cover reduces detection of active fire, as does obscuration of low-intensity surface fires burning in closed canopy forests (Mathews et al., 2016; Morton et al., 2013). Underdetections include small fires that are entirely missed, portions of large fires between potential hot pixel detects that go unobserved, and significant (particularly peak) fire activity that occurs between co-located hot pixel detects in time. These overlapping detections often represent a large proportion of the total energy released but are missed in the subsequent integration of FRE from the undersampled FRP record (Hudak et al., 2015).

A more accurate approach to FRE estimation is to increase fire detections, ideally via high-rate sampling, as is accomplished by geostationary satellites that provide high-rate imaging capability, but at a low spatial resolution (O'Neill et al., 2021; Roberts & Wooster, 2008). O'Neill and Raffuse (2021) demonstrate the use of the U.S. Geostationary Operational Environmental Satellite (GOES) Advanced Baseline Imager (ABI) on the GOES-16 platform to detect fires, compute FRE (see equation 5.3) and estimate emissions using the FEER approach (Ichoku & Ellison, 2014). This approach provides a look at the active fire every 5 min, which allowed modeling of near-surface 1 hr average particulate matter concentrations using an atmospheric dispersion model for the 2020 California Camp wildfire. Limitations include less precise location information and obscuration of the signal by smoke and tree canopies, as previously discussed, but advantages are a more complete accounting of active fire over time. For energetic, fast-moving fires, geostationary-derived information is a major advantage. As techniques to use the high sample-rate data from satellites such as GOES are developed, improvements in smoke tracking and near-real-time forecasting is becoming a reality, as covered in detail in Chapter 9.

5.4.3. Additional Sources of Uncertainty for Mapping Consumption and Emissions.

Developing a realistic estimate of consumption during biomass burning, for both the direct, FRP-based approach and the indirect consumption modeling approach, requires many assumptions due to the complexity of the variables involved. Uncertainty arises from subscale variability in fuels and combustion for both approaches. O'Brien et al. (2016) has shown submeter spatial variation in FRE during fuel combustion. For instance, the FRE of pine cones versus grass fuels in the fuelbed dramatically differs within a 1 m x 1 m microplot, as would the expected emissions. Indeed, inaccurately counting the number of pine cones per meter would dramatically bias emissions estimates, and the same could be said for inaccurate estimations of surface litter loading, duff depth, and other fuel components. Fuel moisture also influences combustion and FRE (Smith et al., 2013), which can change quickly over short timescales as well as spatially. Moisture conditions can be especially impactful in peat-dominated sites, where the water table is an important driver of surface fuel consumption (Bourgeau-Chavez et al., 2020). Most, if not all, fuel components and their moisture content are exceedingly difficult to quantify at the fine scale at which they fundamentally vary, making fuel combustion, even if accounting for vegetation type, one of the largest sources of uncertainty in emissions modeling.

The collective uncertainties in consumption, by either the indirect or direct method, may seem to limit the ability to make reasonable estimates, but factors operating at broader scales serve to constrain fuel loading, consumption, and emissions such that accurate estimates can be derived at higher levels of aggregation. This is not to say that current estimates are necessarily biased, but imprecise at fine scale where fine-scale heterogeneity in fuels and consumption is insufficiently captured. Fuel maps necessarily rely on remote sensing data and empirical models that exploit the statistical relationships between ancillary data provided by remote sensing observables (e.g., spectral reflectance) and the biophysical attributes of interest measured on the ground (e.g., fuels). Such model-based approaches can use bootstrapping of the training data to generate variation in the mapped estimates, which provides a measure of model uncertainty at the pixel level (Urbazaev et al., 2018). Ideally, fuel maps would fully account for all sources of error (sampling, allometric, observation, etc.) that propagate to contribute to overall uncertainty at the pixel level (e.g., LANDFIRE at 30 m resolution). Fully accounting for these cumulative errors remains a challenge (Saatchi et al., 2011); however, in practical terms, much of the fine-scale fuels variation averages out upon aggregation (Bell et al., 2018) to the decision space that typically corresponds to entire fire events and resulting emissions.

5.5. SUMMARY AND CONCLUSIONS

In summary, quantifying emissions from biomass burning is complex and inexact, involves observations and modeling tools, and has matured rapidly in the past three decades (Kasischke & Penner, 2004; Larkin et al., 2020; van der Werf et al., 2017). Emission estimates are needed for quantifying the constituents of pollution found in smoke to address air quality concerns. An emissions inventory provides the data needed to run smoke models that can be integrated into air quality maps and used in decision-making and policy development. Many such models are used for both air quality and climate research and applications. Two approaches are in use to estimate consumption. The indirect approach uses a model-based framework for consumption based on knowledge of fuels and conditions, while the direct approach provides real-time assessment of active fire and calculation of emissions given specific assumptions on combustion. All emissions models suffer inaccuracies from lack of complete knowledge of the fire environment; however, new observational methods are under development that will improve this knowledge to better quantify the emissions originating from biomass burning.

ACKNOWLEDGMENTS

This research was supported by the USDA Forest Service, Rocky Mountain Research Station (AH). The findings and conclusions in this publication are those of the authors and should not be construed to represent any official USDA or United States government determination or policy.

REFERENCES

Akagi, S. K., Yokelson, R. J., Wiedinmyer, C., Alvarado, M. J., Reid, J. S., Karl, T., et al. (2011). Emission factors for open and domestic biomass burning for use in atmospheric models. *Atmospheric Chemistry and Physics, 11*(9), 4039–4072. https://doi.org/10.5194/acp-11-4039-2011

Andreae, M. O. (2019). Emission of trace gases and aerosols from biomass burning – an updated assessment. *Atmospheric Chemistry and Physics, 19*(13), 8523–8546. https://doi.org/10.5194/acp-19-8523-2019

Andreae, M. O., & Merlet, P. (2001). Emission of trace gases and aerosols from biomass burning. *Global Biogeochemical Cycles, 15*(4), 955–966. https://doi.org/10.1029/2000GB001382

Bell, D. M., Gregory, M. J., Kane, V., Kane, J., Kennedy, R. E., Roberts, H. M., et al. (2018). Multiscale divergence between Landsat-and lidar-based biomass mapping is related to regional variation in canopy cover and composition. *Carbon Balance and Management, 13*(1), 1–14.

Boschetti, L., & Roy, D. P. (2009). Strategies for the fusion of satellite fire radiative power with burned area data for fire radiative energy derivation. *Journal of Geophysical Research, 114*(D20302). https://doi.org/10.1029/2008JD011645

Bourgeau-Chavez, L. L., Grelik, S. L., Billimire, M. G., Jenkins, L., Kasischke, E. S., & Turetsky, M. R. (2020). Mapping boreal peatland fire severity and assessing their potential vulnerability to early season wildland fire. *Frontiers in Forests and Global Change, 3*(20). https://doi.org/10.3389/ffgc.2020.00020

Bowman, D. M. J. S., Balch, J. K., Artaxo, P., Bond, W. J., Carlson, J. M., Cochrane, M. A., et al. (2009). Fire in the Earth system. *Science, 324*(5926), 481–484. https://doi.org/10.1126/science.1163886

Byun, D., & Schere, K. L. (2006). Review of the governing equations, computational algorithms, and other components of the Models-3 Community Multiscale Air Quality (CMAQ) modeling system. *Applied Mechanics Reviews, 59*(2), 51–77. https://doi.org/10.1115/1.2128636

Carlson, J., Bradshaw, L. S., Nelson, R. M., Bensch, R. R., & Jabrzemski, R. (2007). Application of the Nelson model to four timelag fuel classes using Oklahoma field observations: Model evaluation and comparison with National Fire Danger Rating System algorithms. *International Journal of Wildland Fire, 16*(2), 204–216. https://doi.org/10.1071/WF06073

Chowdhury, E. H., & Hassan, Q. K. (2015). Operational perspective of remote sensing-based forest fire danger forecasting systems. *ISPRS Journal of Photogrammetry and Remote Sensing, 104*, 224–236. https://doi.org/10.1016/j.isprsjprs.2014.03.011

Cochrane, M. A., Alencar, A., Schulze, M. D., Souza, C. M., Nepstad, D. C., Lefebvre, P., et al. (1999). Positive feedbacks in the fire dynamic of closed canopy tropical forests. *Science, 284*(5421), 1832–1835. https://doi.org/10.1126/science.284.5421.1832

de Groot, W. J., Pritchard, J., & Lynham, T. J. (2009). Forest floor fuel consumption and carbon emissions in Canadian boreal forest fires. *Canadian Journal of Forest Research, 39*, 367–382. https://doi.org/10.1139/X08-192

Dickinson, M. B., Hudak, A. T., Zajkowski, T., Loudermilk, E. L., Schroeder, W., Ellison, L., et al. (2016). Measuring radiant emissions from entire prescribed fires with ground, airborne and satellite sensors: RxCADRE 2012. *International Journal of Wildland Fire, 25*(1), 48. https://doi.org/10.1071/wf15090

Dozier, J. (1981). A method for satellite identification of surface temperature fields of sub-pixel resolution. *Remote Sensing of Environment, 11*, 221–229. https://doi.org/10.1016/0034-4257(81)90021-3

European Environment Agency (2019). *Trends and drivers of EU greenhouse gas emissions*. Luxembourg: Publications Office of the European Union. https://www.eea.europa.eu/publications/trends-and-drivers-of-eu-ghg/download.

Finney, M. A. (1998). *FARSITE: Fire Area Simulator. Model development and evaluation, Report RMRS-RP-4*, (RMRS-RP-4. Fort Collins, CO: U.S. Department of Agriculture, Forest Service, Rocky Mountain Research Station.

Fortin, M. (2021). Comparison of uncertainty quantification techniques for national greenhouse gas inventories. *Mitigation* *and Adaptation Strategies for Global Change*, *26*(2), 7. https://doi.org/10.1007/s11027-021-09947-4

French, N. H. F., Goovaerts, P., & Kasischke, E. S. (2004). Uncertainty in estimating carbon emissions from boreal forest fires. *Journal of Geophysical Research*, *109*, D14S08. https://doi.org/10.1029/2003JD003635

French, N. H. F., Kasischke, E. S., & Williams, D. G. (2002). Variability in the emission of carbon-based trace gases from wildfire in the Alaska boreal forest. *Journal of Geophysical Research*, *107*, 8151. https://doi.org/10.1029/2001JD000480

French, N. H. F., McKenzie, D., Erickson, T., Koziol, B., Billmire, M., Endsley, K. A., et al. (2014). Modeling regional-scale fire emissions with the Wildland Fire Emissions Information System. *Earth Interactions*, *18*, 1–26. https://doi.org/10.1175/EI-D-14-0002.1

Frost, G. J., Middleton, P., Tarrasón, L., Granier, C., Guenther, A., Cardenas, B., et al. (2013). New directions: GEIA's 2020 vision for better air emissions information. *Atmospheric Environment*, *81*, 710–712. https://doi.org/10.1016/j.atmosenv.2013.08.063

Giglio, L., Kendall, J. D., & Mack, R. (2003). A multi-year active fire dataset for the tropics derived from the TRMM VIRS. *International Journal of Remote Sensing*, *24*(22), 4505–4525. https://doi.org/10.1080/0143116031000070283

Giglio, L., Randerson, J., & van der Werf, G. (2013). Analysis of daily, monthly, and annual burned area using the fourth generation Global Fire Emissions Database (GFED4). *Journal of Geophysical Research.* https://doi.org/10.1002/jgrg.20042.c

Giglio, L., van der Werf, G. R., Randerson, J. T., Collatz, G. J., & Kasibhatla, P. (2006). Global estimation of burned area using MODIS active fire observations. *Atmospheric Chemistry and Physics*, *6*, 957–974. https://doi.org/10.5194/acp-6-957-2006

Gurney, K. R., Liang, J., Patarasuk, R., Song, Y., Huang, J., & Roest, G. (2020). The Vulcan Version 3.0 high-resolution fossil fuel CO_2 emissions for the United States. *Journal of Geophysical Research: Atmospheres*, *125*(19). https://doi.org/10.1029/2020jd032974

Hall, J. V., Loboda, T. V., Giglio, L., & McCarty, G. W. (2016). A MODIS-based burned area assessment for Russian croplands: Mapping requirements and challenges. *Remote Sensing of Environment*, *184*, 506–521. https://doi.org/10.1016/j.rse.2016.07.022

Hawbaker, T. J., Vanderhoof, M. K., Schmidt, G. L., Beal, Y.-J., Picotte, J. J., Takacs, J. D., et al. (2020). The Landsat Burned Area algorithm and products for the conterminous United States. *Remote Sensing of Environment*, *244*, 111801. https://doi.org/10.1016/j.rse.2020.111801

Hoelzemann, J. J., Schultz, M. G., Brasseur, G. P., Granier, C., & Simon, M. (2004). Global Wildland Fire Emission Model (GWEM): Evaluating the use of global area burnt satellite data. *Journal of Geophysical Research-Atmospheres*, *109*(D14), D14S04. https://doi.org/10.1029/2003JD003666.

Hoffa, E. A., Ward, D., Hao, W., Susott, R., & Wakimoto, R. (1999). Seasonality of carbon emissions from biomass burning in a Zambian savanna. *Journal of Geophysical Research*, *104*(D11), 13841–13853. https://doi.org/10.1029/1999JD900091

Holder, A. (2019). An overview of the wildland fire emissions inventory at EPA. https://cfpub.epa.gov/si/si_public_record_report.cfm?Lab=CEMM&dirEntryId=348217

Huang, Y., Wu, S., Dubey, M. K., & French, N. H. F. (2013). Impact of aging mechanism on model simulated carbonaceous aerosols. *Atmospheric Chemistry and Physics*, *13*(13), 6329–6343. https://doi.org/10.5194/acp-13-6329-2013

Hudak, A. T., Dickinson, M. B., Bright, B. C., Kremens, R. L., Loudermilk, E. L., O'Brien, J. J., et al. (2015). Measurements relating fire radiative energy density and surface fuel consumption: RxCADRE 2011 and 2012. *International Journal of Wildland Fire*, *25*(1), 25–37. https://doi.org/10.1071/WF14159

Hudak, A. T., Fekety, P. A., Kane, V. R., Kennedy, R. E., Filippelli, S. K., Falkowski, M. J., et al. (2020). A carbon monitoring system for mapping regional, annual aboveground biomass across the northwestern USA. *Environmental Research Letters*, *15*(9), 095003. https://doi.org/10.1088/1748-9326/ab93f9

Hudak, A. T., Lefsky, M. A., Cohen, W. B., & Berterretche, M. (2002). Integration of lidar and Landsat ETM+ data for estimating and mapping forest canopy height. *Remote Sensing of Environment*, *82*(2–3), 397–416. https://doi.org/10.1016/S0034-4257(02)00056-1

Hyer, E. J., & Reid, J. S. (2009). Baseline uncertainties in biomass burning emission models resulting from spatial error in satellite active fire location data. *Geophysical Research Letters*, *36*. https://doi.org/10.1029/2008GL037145

Ichoku, C., & Ellison, L. (2014). Global top-down smoke-aerosol emissions estimation using satellite fire radiative power measurements. *Atmospheric Chemistry and Physics*, *14*(13), 6643–6667. https://doi.org/10.5194/acp-14-6643-2014

IPCC. (2007). *2006 IPCC guidelines for national greenhouse gas inventories*. http://www.ipcc-nggip.iges.or.jp/public/2006gl/index.html

Ito, A., & Penner, J. E. (2004). Global estiamtes of biomass burning emissions based on satellite imagery for the year 2000. *Journal of Geophysical Research*, *109*, D14S05. https://doi.org/10.1029/2003JD004423

Johnston, J. M., Johnston, L. M., Wooster, M. J., Brookes, A., McFayden, C., & Cantin, A. S. (2018). Satellite detection limitations of sub-canopy smouldering wildfires in the North American boreal forest. *Fire*, *1*(2), 28. https://doi.org/10.3390/fire1020028

Kaiser, J. W., Heil, A., Andreae, M. O., Benedetti, A., Chubarova, N., Jones, L., et al. (2012). Biomass burning emissions estimated with a global fire assimilation system based on observed fire radiative power. *Biogeosciences*, *9*(1), 527–554. https://doi.org/10.5194/bg-9-527-2012

Kasischke, E. S., & Penner, J. E. (2004). Improving global estimates of atmospheric emissions from biomass burning. *Journal of Geophysical Research-Atmospheres*, *109*(D14), D14S01. https://doi.org/10.1029/2004JD004972

Kaufman, Y. J., Justice, C. O., Flynn, L. P., Kendall, J. D., Prins, E. M., Giglio, L., et al. (1998). Potential global fire monitoring from EOS-MODIS. *Journal of Geophysical Research: Atmospheres*, *103*(D24), 32215–32238.

Keane, R. E. (2012). Describing wildland surface fuel loading for fire management: A review of approaches, methods and systems. *International Journal of Wildland Fire*, *22*(1), 51–62. https://doi.org/10.1071/WF11139

Keane, R. E. (2015). Surface and ground fuels. In *Wildland fuel fundamentals and applications* (pp. 39–56). Springer.

Keane, R. E., Gray, K., Bacciu, V., & Leirfallom, S. (2012). Spatial scaling of wildland fuels for six forest and rangeland ecosystems of the northern Rocky Mountains, USA. *Landscape Ecology*, *27*(8), 1213–1234. https://doi.org/10.1007/s10980-012-9773-9

Kennedy, R. E., Ohmann, J., Gregory, M., Roberts, H., Yang, Z., Bell, D. M., et al. (2018). An empirical, integrated forest biomass monitoring system. *Environmental Research Letters*, *13*(2), 025004. https://doi.org/10.1088/1748-9326/aa9d9e

Key, C. H., & Benson, N. C. (2006). *Landscape analysis (LA) sampling and analysis methods, RMRS-GTR-164-CD*.

Klauberg, C., Hudak, A., Bright, B., Boschetti, L., Dickinson, M., Kremens, R., et al. (2018). Use of ordinary kriging and Gaussian conditional simulation to interpolate airborne fire radiative energy density estimates. *International Journal of Wildland Fire*, *27*(4), 228–240. https://doi.org/10.1071/WF17113

Kleinman, L. I., Sedlacek, A. J., III, Adachi, K., Buseck, P. R., Collier, S., Dubey, M. K., et al. (2020). Rapid evolution of aerosol particles and their optical properties downwind of wildfires in the western U.S. *Atmospheric Chemistry and Physics*, *20*(21), 13319–13341. https://doi.org/10.5194/acp-20-13319-2020

Knorr, W., Lehsten, V., & Arneth, A. (2012). Determinants and predictability of global wildfire emissions. *Atmospheric Chemistry and Physics*, *12*(15), 6845–6861. https://doi.org/10.5194/acpd-12-4243-2012

Korontzi, S. (2005). Seasonal patterns in biomass burning emissions from southern African vegetation fires for the year 2000. *Global Change Biology*, *11*(10), 1680–1700. https://doi.org/10.1111/j.1365-2486.2005.001024.x

Larkin, N., & O'Neill, S. M. (2018). *BlueSky playground v 3.5*. https://info.airfire.org/playground

Larkin, N. K., O'Neill, S. M., Solomon, R., Raffuse, S., Strand, T., Sullivan, D. C., et al. (2009). The BlueSky smoke modeling framework. *International Journal of Wildland Fire*, *18*(8), 906–920. https://doi.org/10.1071/WF07086

Larkin, N. K., Raffuse, S. M., Huang, S., Pavlovic, N., Lahm, P., & Rao, V. (2020). The comprehensive fire information reconciled emissions (CFIRE) inventory: Wildland fire emissions developed for the 2011 and 2014 U.S. National Emissions Inventory. *Journal of the Air and Waste Management Association*, *70*(11), 1165–1185. https://doi.org/10.1080/10962247.2020.1802365

Leite, R. V., Silva, C. A., Broadbent, E. N., Do Amaral, C. H., Liesenberg, V., De Almeida, D. R. A., et al. (2022). Large scale multi-layer fuel load characterization in tropical savanna using GEDI spaceborne lidar data. *Remote Sensing of Environment*, *268*, 112764.

Levine, J. S. (Ed.) (1991). *Global biomass burning: Atmospheric, climatic, and biospheric implications*. Cambridge, MA: MIT Press.

Mathews, B. J., Strand, E. K., Smith, A. M., Hudak, A. T., Dickinson, B., & Kremens, R. L. (2016). Laboratory experiments to estimate interception of infrared radiation by tree canopies. *International Journal of Wildland Fire*, *25*(9), 1009–1014. https://doi.org/10.1071/WF16007

McCarley, T. R., Hudak, A. T., Sparks, A. M., Vaillant, N. M., Meddens, A. J. H., Trader, L., et al. (2020). Estimating wildfire fuel consumption with multitemporal airborne laser scanning data and demonstrating linkage with MODIS-derived fire radiative energy. *Remote Sensing of Environment*, *251*, 112114. https://doi.org/10.1016/j.rse.2020.112114

McCarty, J. L., Aalto, J., Paunu, V.-V., Arnold, S. R., Eckhardt, S., Klimont, Z., et al. (2021). Reviews and syntheses: Arctic fire regimes and emissions in the 21st century. *Biogeosciences*, *18*(18), 5053–5083. https://doi.org/10.5194/bg-18-5053-2021

Michalek, J. L., French, N. H. F., Kasischke, E. S., Johnson, R. D., & Colwell, J. E. (2000). Using Landsat TM data to estimate carbon release from burned biomass in an Alaskan spruce complex. *International Journal of Remote Sensing*, *21*(2), 323–338. https://doi.org/10.1080/014311600210858

Morton, D., Le Page, Y., DeFries, R., Collatz, G., & Hurtt, G. (2013). Understorey fire frequency and the fate of burned forests in southern Amazonia. *Philosophical Transactions of the Royal Society B: Biological Sciences*, *368*(1619), 20120163. https://doi.org/10.1098/rstb.2012.0163

Morton, D. C., DeFries, R. S., Nagol, J., Souza, C. M., Jr., Kasischke, E. S., Hurtt, G. C., et al. (2011). Mapping canopy damage from understory fires in Amazon forests using annual time series of Landsat and MODIS data. *Remote Sensing of Environment*, *115*(7), 1706–1720. https://doi.org/10.1016/j.rse.2011.03.002

Nelson, R. M., Jr. (2000). Prediction of diurnal change in 10-h fuel stick moisture content. *Canadian Journal of Forest Research*, *30*(7), 1071–1087. https://doi.org/10.1139/x00-032

Nelson, R. M., Jr. (2001). Water relations of forest fuels. In E. A. Johnson & K. Miyanishi (Eds.), *Forest fires: Behavior and ecological effects*, (pp. 79–149). San Diego, CA: Academic Press.

NOAA (2021). *Fire influence on regional to global environments and air quality (FIREX-AQ)*. https://csl.noaa.gov/projects/firex-aq/

O'Brien, J. J., Loudermilk, E. L., Hiers, J. K., Pokswinski, S. M., Hornsby, B., Hudak, A. T., et al. (2016). Canopy-derived fuels drive patterns of in-fire energy release and understory plant mortality in a longleaf pine (*Pinus palustris*) sandhill in northwest Florida, USA. *Canadian Journal of Remote Sensing*, *42*(5), 489–500. https://doi.org/10.1080/07038992.2016.1199271

O'Neill, S., & Raffuse, S. (2021). Advances in satellite data for wildfire smoke forecasting. *EOS*, *102*. https://doi.org/10.1029/2021EO155076

O'Neill, S. M., Diao, M., Raffuse, S., Al-Hamdan, M., Barik, M., Jia, Y., et al. (2021). A multi-analysis approach for estimating regional health impacts from the 2017 Northern California wildfires. *Journal of the Air and Waste Management Association*, *71*(7), 791–814. https://doi.org/10.1080/10962247.2021.1891994

Olson, J. S. (1963). Energy storage and the balance of producers and decomposers in ecological systems. *Ecology*, *44*(2), 322–331.

Ottmar, R. D. (2014). Wildland fire emissions, carbon, and climate: Modeling fuel consumption. *Forest Ecology and*

Management, *317*, 41–50. https://doi.org/10.1016/j.foreco.2013.06.010

Ottmar, R. D., Sandberg, D. V., Riccardi, C. L., & Prichard, S. J. (2007). An overview of the Fuel Characteristic Classification System (FCCS): Quantifying, classifying, and creating fuelbeds for resource planning. *Canadian Journal of Forest Research*, *37*, 2383–2393. https://doi.org/10.1139/X07-077

Pettinari, M. L., & Chuvieco, E. (2016). Generation of a global fuel data set using the Fuel Characteristic Classification System. *Biogeosciences*, *13*(7), 2061–2076. https://doi.org/10.5194/bg-13-2061-2016

Pettinari, M. L., Ottmar, R. D., Prichard, S. J., Andreu, A. G., & Chuvieco, E. (2013). Development and mapping of fuel characteristics and associated fire potentials for South America. *International Journal of Wildland Fire*. https://doi.org/10.1071/WF12137

Pfister, G. G., Avise, J., Wiedinmyer, C., Edwards, D. P., Emmons, L. K., Diskin, G. D., et al. (2011). CO source contribution analysis for California during ARCTAS-CARB. *Atmospheric Chemistry and Physics*, *11*(15), 7515–7532. https://doi.org/10.5194/acp-11-7515-2011

Popescu, S., Wynne, R., & Nelson, R. (2003). Measuring individual tree crown diameter with lidar and assessing its influence on estimating forest volume and biomass. *Canadian Journal of Remote Sensing*, *29*(5), 564–577. https://doi.org/10.5589/m03-027

Pouliot, G., Pace, T. G., Roy, B., Pierce, T., & Mobley, D. (2008). Development of a biomass burning emissions inventory by combining satellite and ground-based information. *Journal of Applied Remote Sensing*, *2*(16 May 2008), 021501. https://doi.org/10.1117/1.2939551

Prichard, S. J., Keane, R., Rowell, E., Hudak, A., Loudermilk, E. L., Lutes, D., et al. (2021). Fuels and consumption. In D. L. Peterson, S. M. McCaffrey, & T. Patel-Weyand (Eds.), *U.S. Forest Service national smoke assessment*. Springer.

Prichard, S. J., Kennedy, M. C., Andreu, A. G., Eagle, P., & French, N. H. F. (2019). Next-generation biomass mapping for regional emissions and carbon inventories: Incorporating uncertainty in wildland fuel characterization. *Journal of Geophysical Research*, *134*. https://doi.org/10.1029/2019JGR005083

Prichard, S. J., O'Neill, S. M., Eagle, P., Andreu, A. G., Drye, B., Dubowy, J., et al. (2020). Wildland fire emission factors in North America: Synthesis of existing data, measurement needs and management applications. *International Journal of Wildland Fire*, *29*(2), 132–147. https://doi.org/10.1071/WF19066

Prichard, S. J., Ottmar, R. D., & Anderson, G. A. (2009). *CONSUME 3.0 users guide*. Pacific Wildland Fire Sciences Laboratory, USDA Forest Service. Seattle, WA. http://www.fs.fed.us/pnw/fera/research/smoke/consume/consume30_users_guide.pdf

Prichard, S. J., Ottmar, R. D., & Anderson, G. K. (2006). *CONSUME 3.0 user's guide*. Fire and Environmental Research Applications Team, USDA Forest Service. Seattle, WA. http://www.fs.fed.us/pnw/fera/research/smoke/consume/consume30_users_guide.pdf

Randerson, J. T., Chen, Y., van der Werf, G. R., Rogers, B. M., & Morton, D. C. (2012). Global burned area and biomass burning emissions from small fires. *Journal of Geophysical Research: Biogeosciences*, *117*(G4), n/a-n/a. https://doi.org/10.1029/2012JG002128

Rappold, A. G., Stone, S. L., Cascio, W. E., Neas, L. M., Kilaru, V. J., Carraway, M. S., et al. (2011). Peat bog wildfire smoke exposure in rural North Carolina is associated with cardiopulmonary emergency department visits assessed through syndromic surveillance. *Environmental Health Perspectives*, *119*(10), 1415–1420.

Reid, J. S., Hyer, E. J., Prins, E. M., Westphal, D. M., Zhang, J., Wang, J., et al. (2009). Global monitoring and forecasting of biomass-burning smoke: Description of and lessons from the Fire Locating and Modeling of Burning Emissions (FLAMBE) program. *IEEE Journal of Selected Topics in Applied Earth Observations and Remote Sensing*, *2*(3). https://doi.org/10.1109/JSTARS.2009.2027443

Reinhardt, E. D., Keane, R. E., & Brown, J. K. (1997). *First Order Fire Effects Model: FOFEM 4.0, user's guide*. USDA Forest Service, General Technical Report INT- GTR-344.

Roberts, G., Wooster, M., Freeborn, P., & Xu, W. (2011). Integration of geostationary FRP and polar-orbiter burned area datasets for an enhanced biomass burning inventory. *Remote Sensing of Environment*, *115*(8), 2047–2061. https://doi.org/10.1016/J.RSE.2011.04.006

Roberts, G. J., & Wooster, M. J. (2008). Fire detection and fire characterization over Africa using Meteosat SEVIRI. *IEEE Transactions on Geoscience and Remote Sensing*, *46*(4), 1200–1218. https://doi.org/10.1109/TGRS.2008.915751

Rollins, M. G. (2009). LANDFIRE: A nationally consistent vegetation, wildland fire, and fuel assessment. *International Journal of Wildland Fire*, *18*(3), 235–249. https://doi.org/10.1071/WF08088

Saatchi, S. S., Harris, N. L., Brown, S., Lefsky, M., Mitchard, E. T., Salas, W., et al. (2011). Benchmark map of forest carbon stocks in tropical regions across three continents. *Proceedings of the National Academy of Sciences*, *108*(24), 9899–9904.

Schultz, M. G., Heil, A., Hoelzemann, J. J., Spessa, A., Thonicke, K., Goldammer, J. G., et al. (2008). Global wildland fire emissions from 1960 to 2000. *Global Biogeochemical Cycles*, *22*. https://doi.org/10.1029/2007GB003031

Seiler, W., & Crutzen, P. J. (1980). Estimates of gross and net fluxes of carbon between the biosphere and atmosphere from biomass burning. *Climatic Change*, *2*, 207–247.

Seinfeld, J. H., & Pandis, S. N. (1998). *Atmospheric chemistry and physics: From air pollution to climate change*. New York: John Willey & Sons.

Selimovic, V., Yokelson, R. J., McMeeking, G. R., & Coefield, S. (2019). In situ measurements of trace gases, PM, and aerosol optical properties during the 2017 NW U.S. wildfire smoke event. *Atmospheric Chemistry and Physics*, *19*(6), 3905–3926. https://doi.org/10.5194/acp-19-3905-2019

Skowronski, N., Clark, K., Nelson, R., Hom, J., & Patterson, M. (2007). Remotely sensed measurements of forest structure and fuel loads in the Pinelands of New Jersey. *Remote Sensing of Environment*, *108*(2), 123–129. https://doi.org/10.1016/j.rse.2006.09.032

Smith, A. M. S., Tinkham, W. T., Roy, D. P., Boschetti, L., Kremens, R. L., Kumar, S. S., et al. (2013). Quantification of fuel moisture effects on biomass consumed derived from fi...

radiative energy retrievals. *Geophysical Research Letters*, *40*, 6298–6302. https://doi.org/10.1002/2013GL058232

Souza, J., Carlos, M., Roberts, D. A., & Cochrane, M. A. (2005). Combining spectral and spatial information to map canopy damage from selective logging and forest fires. *Remote Sensing of Environment*, *98*(2–3), 329–343. https://doi.org/10.1016/j.rse.2005.07.013

UNECE (1979). *1979 Convention on Long-range Transboundary Air Pollution*. https://unece.org/convention-and-its-achievements

UNFCCC (2021). *Greenhouse gas reporting requirements*. https://unfccc.int/process-and-meetings/transparency-and-reporting/reporting-and-review-under-the-convention/greenhouse-gas-inventories-annex-i-parties/reporting-requirements

Urbanski, S. (2014). Wildland fire emissions, carbon, and climate: Emission factors. *Forest Ecology and Management*, *317*, 51–60. https://doi.org/10.1016/j.foreco.2013.05.045

Urbanski, S. P., Hao, W. M., & Nordgren, B. (2011). The wildland fire emission inventory: Western United States emission estimates and an evaluation of uncertainty. *Atmospheric Chemistry and Physics*, *11*(24), 12973–13000. https://doi.org/10.5194/acp-11-12973-2011

Urbanski, S. P., O'Neill, S. M., Holder, A. L., Green, S. A., & Graw, R. L. (2021). Emissions. In D. L. Peterson, S. M. McCaffrey, & T. Patel-Weyand (Eds.), *U.S. Forest Service National Smoke Assessment*. Springer.

Urbazaev, M., Thiel, C., Cremer, F., Dubayah, R., Migliavacca, M., Reichstein, M., et al. (2018). Estimation of forest aboveground biomass and uncertainties by integration of field measurements, airborne LiDAR, and SAR and optical satellite data in Mexico. *Carbon Balance and Management*, *13*(1), 1–20.

USEPA (2021a). *Criteria air pollutants*. https://www.epa.gov/criteria-air-pollutants

USEPA (2021b). *U.S. greenhouse gas emissions and sinks: 1990–2019*. https://www.epa.gov/ghgemissions/inventory-us-greenhouse-gas-emissions-and-sinks

USGS (2021). *3D elevation program*. https://www.usgs.gov/core-science-systems/ngp/3dep

Vallack, H. W., & Rypdal, K. (2019). *The global atmospheric pollution forum air pollutant emission inventory manual*, Version 6.0 May 2019 revision: York.

van der Werf, G., Randerson, J. T., Giglio, L., Collatz, G. J., Kasibhatla, P. S., & Arellano, A. F. (2006). Interannual variability of global biomass burning emissions from 1997 to 2004. *Atmospheric Chemistry and Physics*, *6*, 3423–3441. https://doi.org/10.5194/acp-6-3423-2006

van der Werf, G. R., Randerson, J. T., Giglio, L., van Leeuwen, T. T., Chen, Y., Rogers, B. M., et al. (2017). Global fire emissions estimates during 1997–2016. *Earth System Science Data*, *9*(2), 697–720. https://doi.org/10.5194/essd-9-697-2017

van Leeuwen, T., Peters, W., Krol, M., & Van Der Werf, G. (2013). Dynamic biomass burning emission factors and their impact on atmospheric CO mixing ratios. *Journal of Geophysical Research: Atmospheres*, *118*(12), 6797–6815. https://doi.org/10.1002/jgrd.50478

van Leeuwen, T. T. (2014). *Modeling spatio-temporal variability in biomass burning emission factors*. PhD dissertation. Vrije Univeriteit, Amsterdam.

van Leeuwen, T. T., van der Werf, G. R., Hoffmann, A. A., Detmers, R. G., Rücker, G., French, N. H. F., et al. (2014). Biomass burning fuel consumption rates: A field measurement database. *Biogeosciences*, *11*(24), 7305–7329. https://doi.org/10.5194/bg-11-7305-2014

Viegas, D., Piñol, J., Viegas, M., & Ogaya, R. (2001). Estimating live fine fuels moisture content using meteorologically-based indices. *International Journal of Wildland Fire*, *10*(2), 223–240. https://doi.org/doi.org/10.1071/WF01022

Viegas, D., Viegas, M., & Ferreira, A. (1992). Moisture content of fine forest fuels and fire occurrence in central Portugal. *International Journal of Wildland Fire*, *2*(2), 69–86. https://doi.org/10.1071/WF9920069

Viney, N. (1991). A review of fine fuel moisture modelling. *International Journal of Wildland Fire*, *1*(4), 215–234. https://doi.org/10.1071/WF9910215

Wiedinmyer, C., Akagi, S. K., Yokelson, R. J., Emmons, L. K., Al-Saadi, J. A., Orlando, J. J., et al. (2011). The fire inventory from NCAR (FINN): A high resolution global model to estimate the emissions from open burning. *Geoscientific Model Development*, *4*(3), 625–641. https://doi.org/10.5194/gmd-4-625-2011

Wooster, M. J., Roberts, G., Smith, A. M., Johnston, J., Freeborn, P., Amici, S., et al. (2013). Thermal remote sensing of active vegetation fires and biomass burning events. In C. Kuenzer & S. Dech (Eds.), *Thermal infrared remote sensing* (pp. 347–390). Springer.

Wooster, M. J., Robertson, G., Perry, G. L. W., & Kaufman, Y. J. (2005). Retrieval of biomass combustion rates and totals from fire radiative power observations: FRP derivation and calibration relationships between biomass consumption and fire radiative energy release. *Journal of Geophysical Research*, *D24311*. https://doi.org/10.1029/2005JD006318

Wooster, M. J., Zhukov, B., & Oertel, D. (2003). Fire radiative energy for quantitative study of biomass burning: derivation from the BIRF experimental satellite and comparison to MODIS fire products. *Remote Sensing of the Environment*, *86*, 83–107. https://doi.org/10.1016/S0034-4257(03)00070-1

Wulder, M. A., Bater, C. W., Coops, N. C., Hilker, T., & White, J. C. (2008). The role of LiDAR in sustainable forest management. *The Forestry Chronicle*, *84*(6), 807–826. https://doi.org/10.5558/tfc84807-6

Yao, J., Brauer, M., & Henderson, S. B. (2013). Evaluation of a wildfire smoke forecasting system as a tool for public health protection. *Environmental Health Perspectives*, *121*(10), 1142–1147. https://doi.org/10.1289/ehp.1306768

Yebra, M., Dennison, P. E., Chuvieco, E., Riano, D., Zylstra, P., Hunt, E. R., Jr., et al. (2013). A global review of remote sensing of live fuel moisture content for fire danger assessment: Moving towards operational products. *Remote Sensing of Environment*, *136*, 455–468. https://doi.org/10.1016/j.rse.2013.05.029

Yokelson, R. J., Goode, J. G., Ward, D. E., Susott, R. A., Babbitt, R. E., Wade, D. D., et al. (1999). Emissions of formaldehyde, acetic acid, methanol, and other trace gases from biomass fires in North Carolina measured by airborne Fourier transform infrared spectroscopy. *Journal of Geophysical Research: Atmospheres*, *104*(D23), 30109–30125. https://doi.org/10.1029/1999JD900817

Zhang, G., Ganguly, S., Nemani, R. R., White, M. A., Milesi, C., Hashimoto, H., et al. (2014). Estimation of forest aboveground biomass in California using canopy height and leaf area index estimated from satellite data. *Remote Sensing of Environment*, *151*, 44–56. https://doi.org/10.1016/j.rse.2014.01.025

Zhang, X., Kondragunta, S., Da Silva, A., Lu, S., Ding, H., Li, F., & Zhu, Y. (2019). *The Blended global biomass buring emissions product from MODIS and VIIRS observations (GBBEPx), version 3.1.* https://www.ospo.noaa.gov/Products/land/gbbepx/docs/GBBEPx_ATBD.pdf